

Deformations of R.C.Circular Slabs in Fire Condition

A. T. Kassem ^{a*}

^a *Civil Engineering Department, Faculty of engineering / Beni-Suef University, Egypt.*

Received 20 February 2018; Accepted 25 March 2018

Abstract

Reinforced concrete slabs are elements in direct contact with superimposed loads, having high surface area and small thickness. Such a condition makes slabs highly vulnerable to fire conditions. Fire results in exaggerated deformations in reinforced concrete slabs, as a result of material deterioration and thermal induced stresses. The main objective of this paper is to deeply investigate how circular R.C. slabs, of different configurations, behave in fire condition. That objective has been achieved through finite element modelling. Thermal-structural finite element models have been prepared, using "Ansys". Finite element models used solid elements to model both thermal and structural slab behaviour. Structural loads had been applied, representing slab operational loads, then thermal loads were applied in accordance with ISO 843 fire curve. Outputs in the form of deflection profile and edge rotation have been extracted out of the models to present slab deformations. A parametric study has been conducted to figure out the significance of various parameters such as; slab depth, slenderness ratio, load ratio, and opening size; regarding slab deformations. It was found that deformational behaviour differs significantly for slabs of thickness equal or below 100 mm, than slabs of thickness equal or above 200 mm. On the other hand considerable changes in slabs behaviour take place after 30 minutes of fire exposure for slabs of thickness equals or below 100 mm, while such changes delay till 60 minutes for slabs of thickness equals or above 200 mm.

Keywords: R.C; Circular Slabs; Fire Load; Structural Deformations.

1. Introduction

The significance of this research arises from its applications. Circular R.C slabs are widely used in silos and tanks, in either upper or lower slabs. Upper slabs are usually solid, in case of side feeding of tanks: while lower ones are usually concentrically opened to allow content discharge. Deformations of both slabs are significant design parameters, due to installed mechanical equipment, especially around openings. This research concentrates on deformations of circular R.C. slabs, when subjected to a fire load simultaneously with superimposed loads.

The structural problem of circular plates is considered one of the classical structural engineering problems. It has been first been expressed by Timoshenko (1959). Through the free body diagram shown in Figure 1. The presented circular plate problem is axisymmetric, so variation in straining actions and deformations takes place along the radial direction only.

* Corresponding author: abdelraouf_kassem@yahoo.com

 <http://dx.doi.org/10.28991/cej-0309126>

➤ This is an open access article under the CC-BY license (<https://creativecommons.org/licenses/by/4.0/>).

© Authors retain all copyrights.

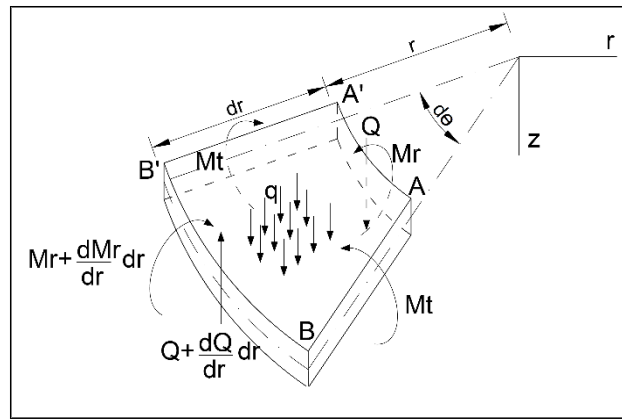


Figure 1. Circular plate free body diagram

A number of recent research have studied reinforced concrete slabs in fire condition. Foster, Burgess, and Plank have investigated effects of thermal curvature on slabs failure mechanisms. They found that slabs do not collapse, even at a high of deformations. This has been explained as a direct effect of tensile membrane forces which enhances structural integrity by diaphragm action. Zhaohui, Burgess, and Plank could model slab tensile membrane action, in fire condition, through a nonlinear multilayered finite element model, prepared based on the thick plate theory. On the other hand Izzuddin has presented a new model, based on flat elements, for nonlinear analysis of reinforced concrete slab systems at extreme loading. This orthotropic model could take into account effects of difference of reinforcement in slabs two perpendicular directions.

Research methodology has been built upon finite element modelling, as common in fire engineering field. Models verification has been implemented for both structural and thermal analyses. Structural verification has been implemented by comparing outputs rising out of models by closed form formulae, available in the literature, for special linear cases. While verification of thermal models has been fulfilled through comparing temperature profile with standard curves available in the literature for a 100 mm thick slab. General closed form formulae for both structural and thermal analysis modules are presented hereinafter.

Deflection for a uniformly distributed axisymmetric loading applied to a simply supported solid circular slab could be expressed by Equation 1.

$$w = \frac{qR^4}{64EI} \left(1 - \left(\frac{x}{R}\right)^4\right)^2 \tag{1}$$

While in case of circular plates with central opening deflection could be expressed as shown in Equation 2.

$$w = \frac{qR^4}{64EI} \left\{ \frac{2}{1+\nu} [(3+\nu)(1+2\beta^2) + k_1](1-\rho^2) - (1-\rho^4) - \frac{4k_1 \ln \rho}{1-\nu} - 8\beta^2 \rho^2 \ln \rho \right\} \tag{2}$$

Where:

- W is the deflection at a specific distance from the centreline.
- Q is the uniformly distributed load
- R is the overall plate radius
- X is the distance from plate centreline to a considered point
- E is the modulus of elasticity
- I is the second moment of area

$$\rho = \frac{x}{R}$$

$$\beta = \frac{D'}{D}$$

$$k_1 = \beta^2 \left[3 + \nu + 4(1 + \nu) \frac{\beta^2}{1 - \beta^2} \ln \beta \right]$$

It should be noted that the previously stated equations are valid only for small deformations, and used only for finite element verification. Large deformations that take place as a result of material deterioration at elevated temperatures, result in tensile membrane action that could be analysed via finite element only.

Since the problem involves single sided thermal loading a transient heat transfer problem could be formulated to evaluate temperature distribution within the concrete slab, as a function of time, as expressed via Equation 3; in case of consistent material properties and linearly varying thermal loading.

$$C_c \frac{dT_c}{dt} = kA \frac{dT}{dx} - hA(T_s - T_a) \tag{3}$$

Where

C_c is the concrete specific heat
 h is the convection heat transfer coefficient
 t is time
 T_s is surface temperature

k_c is the concrete thermal conductivity
 x is the plate thickness
 A is the surface area
 T_a is ambient temperature

Once model had been verified it has been used to solve the thermal analysis. Outputs of thermal analysis, in the form of temperature profile across concrete slab as a function of time have been saved in the model, for two main reasons. The first is determining temperature dependent material properties at each time step of the structural analysis. The second is applying the thermal load to the slab at each time step to determine resulting deformations and straining actions, simultaneously with structural loading, according to loading curve shown hereinafter in Figure 3. Outputs of the finite element model have been included in a parametric study to figure out effects of various structural parameters on deformations of circular slabs with and without central openings. The parametric study has implemented structural and thermal loading patterns for case of solid slabs, to extract deflection profile and for the case of slabs with central opening to extract edge rotation.

2. Finite Element Model

A finite element model has been prepared to model thermal-structural behaviour of concrete circular slabs in fire condition. The model used solid elements, of configuration as shown in Figure 2, capable of running both thermal and structural analyses. The finite element model has been constructed of solid elements, forming the required circular geometry, with a variety of depths, diameters, and central circular openings sizes. Hinged end condition has been assigned along the slab circumference. Results of finite element model have been extracted in the form of deflection profile, for solid slabs, and edge rotation for centrally perforated slabs. Model loading strategy has been prepared based on both structural and thermal loading, as shown in Figure 3.

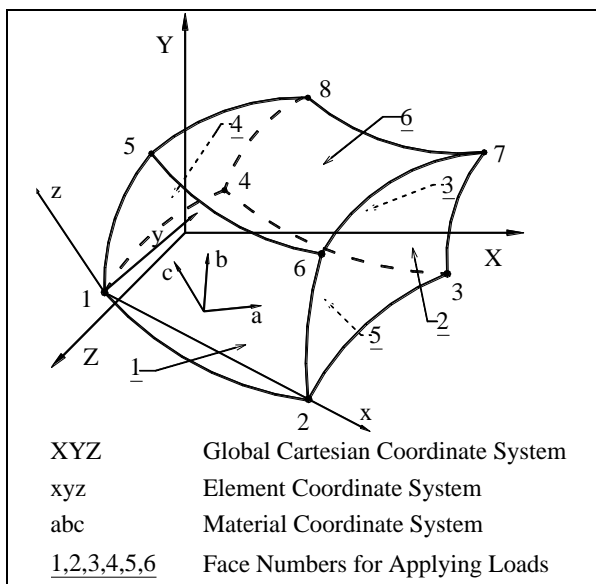


Figure 2. Solid element's configurations

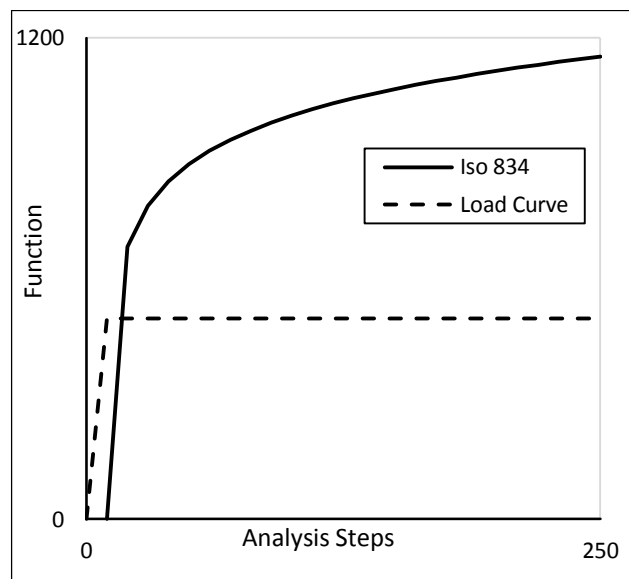


Figure 3. Structural-thermal load curve

The finite element model, used in structural analysis has been prepared to deal with a uniformly distributed, axisymmetric superimposed load, applied to the circular slab as shown in Figure 4-a. Finite element interpretation considering geometry and mesh properties has been implemented as shown in Figure 4-b.

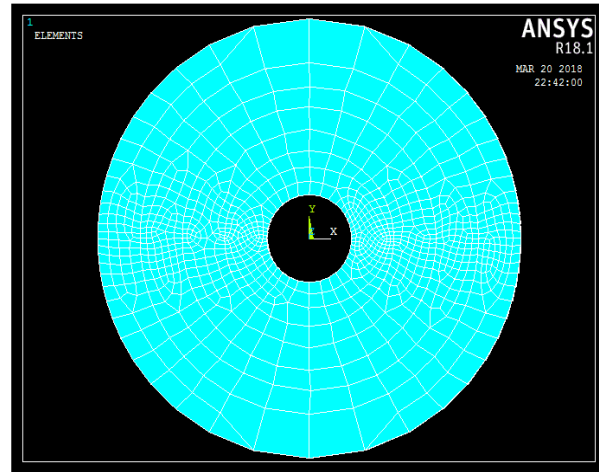
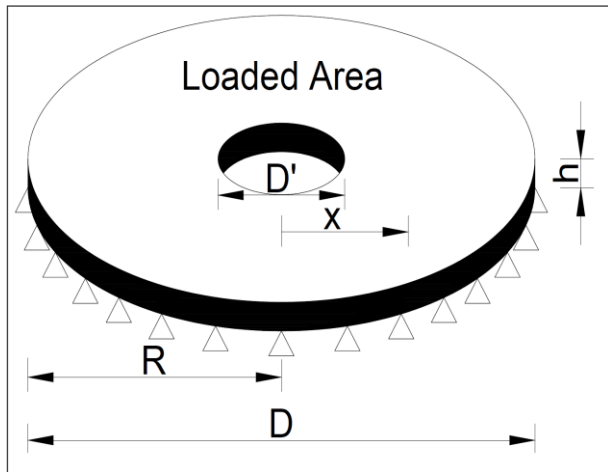


Figure 4-a. Circular slab static system and structural loading

Figure 4-b. Circular slab modelled geometry and meshing

Verification of structural model has been performed in conjunction with the closed form circular plate deflection evaluation formulae, in case of solid and opened circular plates. Structural verification has been performed for the case of having consistent material properties within the whole plate. Verification of thermal model is shown in details in thermal analysis, hereinafter. Figure 5 shows model deflection profiles of the 5000 mm diameter and 100 mm thick slab in case of structural loading.

Finite element modelling procedures, for the structural analysis had begun by applying structural loads, to simulate the initial condition before fire, then fire load was applied in accordance with ISO 834 fire Curve 6. Analysis has been performed on two stages. The first stage was thermal analysis, where fire load had been applied and a transient heat transfer problem was solved. Outputs of the heat transfer problem were then saved in the model. The second stage is application of load curves, previously presented. Load curves began by solving a superimposed uniform load; then the thermal load, previously saved. Outputs regarding thermal-structural deformations were then extracted and saved in a separate file.

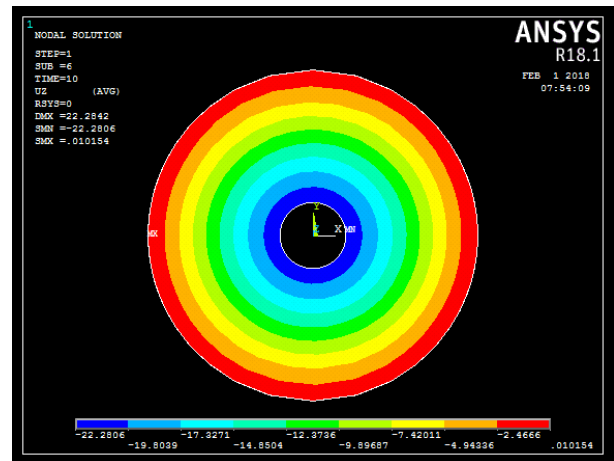
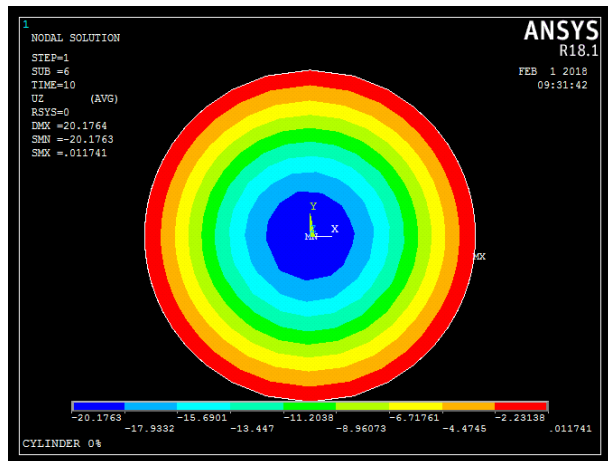


Figure 5-a. Solid circular slab structural loads deflection

Figure 5-b. Slab of 20% opening structural loads deflection

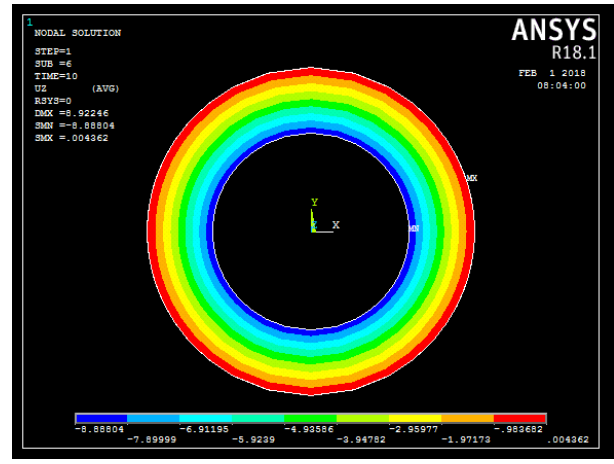
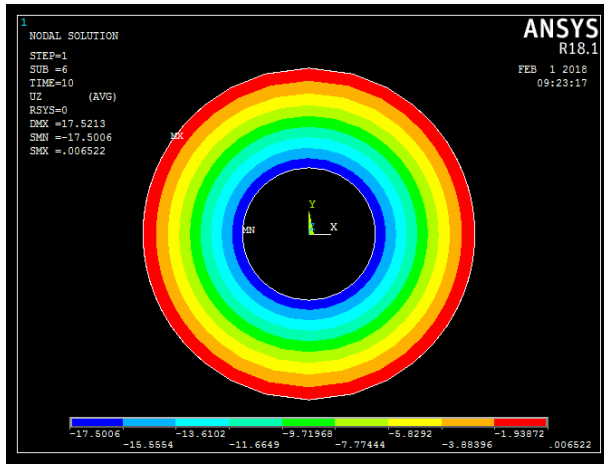


Figure 5-c. Slab of 40% opening structural loads deflection Figure 5-d. Slab of 60% opening structural loads deflection

Figure 5. Deflection of 5000mm diameter, 100mm thick slab after structural load application

3. Thermal Analysis

Thermal analysis of circular slabs has been prepared based on material thermal properties temperature dependency curves stated in EURO Code 6, regarding specific heat and thermal conductivity. Even a three dimensional thermal-structural model has been prepared, but thermal analysis could approximately be expressed uni-dimensionally; due to problem geometry and boundary conditions, as shown in Figure 6. Thermal load has been applied to slab soffit only. This condition forced temperature to flow uni-dimensionally till the upper side of the slab, since no side thermal interference exists. Outputs of slab temperature have been extracted at nodes along the slab depth. Verification of thermal analysis has been established versus temperature diagrams presented in the Euro Code for a 100 mm thick concrete slab and showed sufficient coherence, as shown in Figure 7.

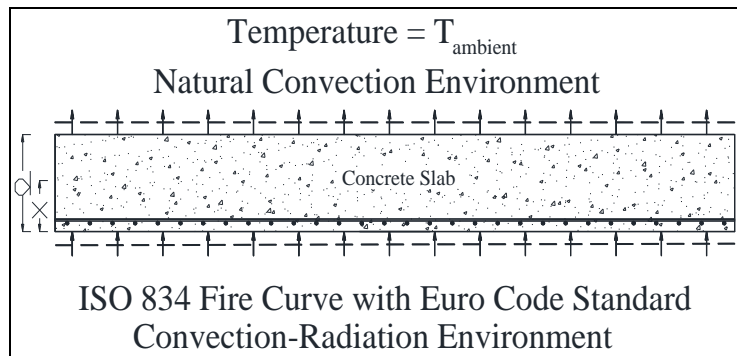


Figure 6. Thermal Problem Boundary conditions

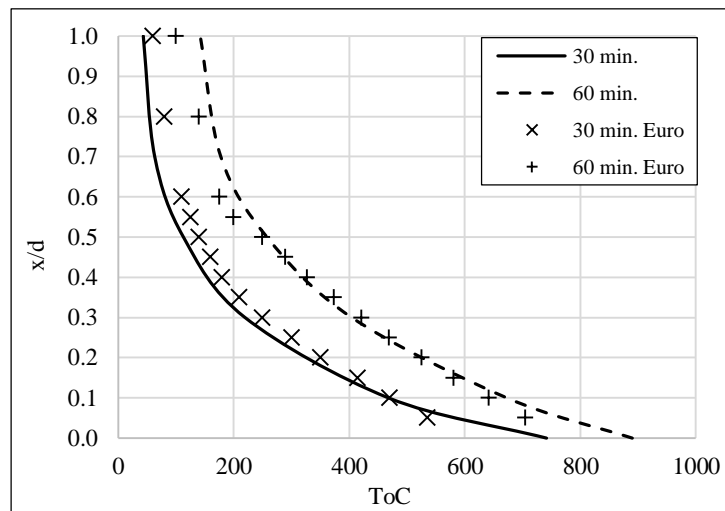


Figure 7. Verification of thermal model versus Euro code

Figures 8 to 11 display temperature profiles across slab depth, as a function of time, beginning by 30 minutes of fire exposure till four hours of fire application. Four different slab thicknesses have been considered (50, 100, 200 and 400 mm).

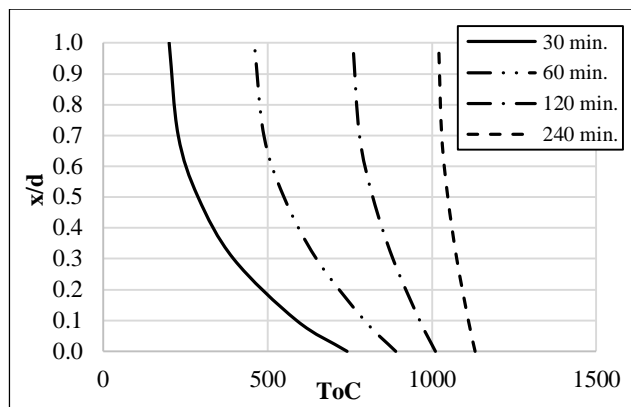


Figure 8. Temperature profile of 50 mm slab thick

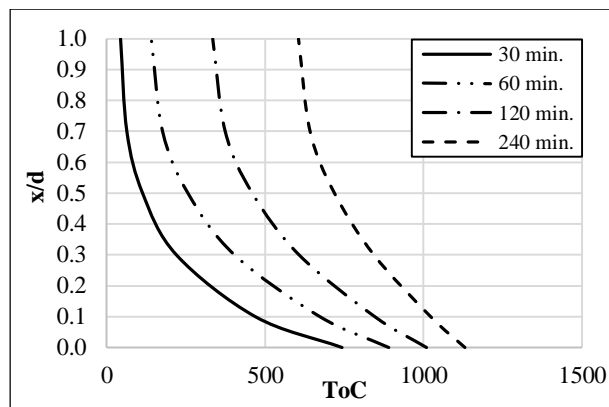


Figure 9. Temperature profile of 100 mm slab thick

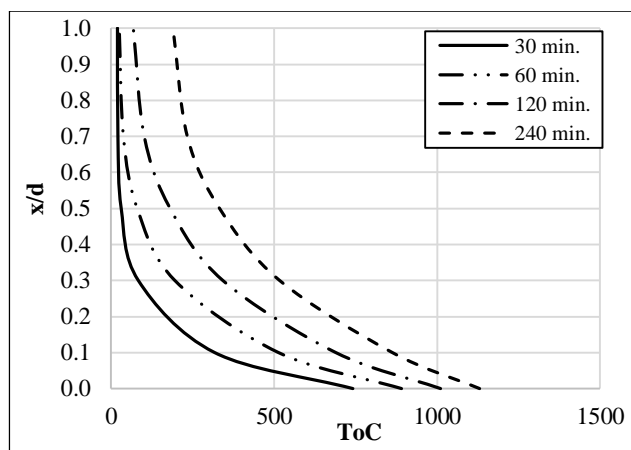


Figure 10. Temperature profile of 200 mm slab thick

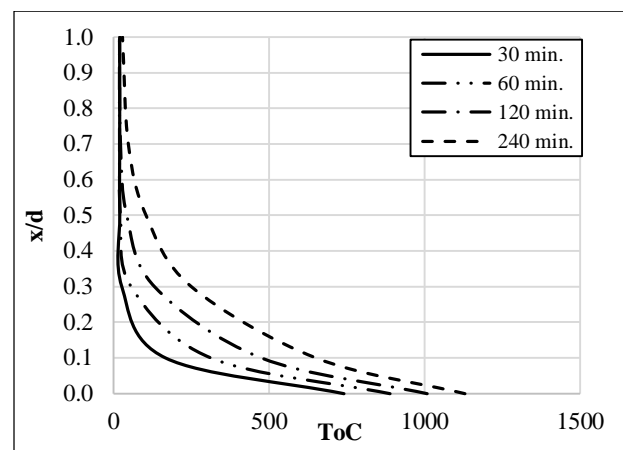


Figure 11. Temperature profile of 400 mm slab thick

It could be noticed that temperature distribution within slab depth is non-linear and dependent on slab total thickness and time. Since thermal analysis has been performed to study structural deformations, both values and differences in temperature between various points are of a significant role. Temperature value is significant, regarding temperature dependent material properties, while difference in temperature, forming thermal profile variation is significant in determining forced deformations. Moreover it could be seen, to what extent temperature profile is highly dependent on slab thickness. The 50 mm slab showed maximum temperature band width from 30 to 60 minutes then temperature spectrum converge till 240 minute. This convergence is a result of the low thermal capacity of the 50 mm deep slab that heated up rapidly till it reached an approximately uniform temperature after four hours of ISO 834 application. On the other hand the 400 mm slab showed minimum temperature band width in the beginning of fire exposure, then divergence took place till it reached a maximum level at 240 minutes of exposure.

4. Parametric Study

A number of models have been prepared to study effects of various structural parameters on the deformations of circular reinforced concrete slabs in fire condition. Four different diameter to depth ratios have been considered ($D/d=25, 50, 100, \text{ and } 200$). Four different opening to diameter ratios have been considered ($D'/D= 0, 20\%, 40\%, \text{ and } 60\%$). Outputs of thermal and structural deformations in the form of deflection profile and edge rotation have been extracted from models for solid and centrally opened slabs.

4.1. Thermal Induced Edge Rotation

Edge rotation has been extracted from slender slab models ($D/d=200$). Rotation for various opening sizes has been plotted on the same graph, as functions of time. The main studied parameters in this case were opening size and slab thickness. It could be noticed that the form of edge rotation graph is highly vulnerable to slab thickness. In case of slim slabs rotation reaches its maximum value between 30 and 60 minutes of fire exposure. This could be attributed to effects of steep temperature distribution within slab depth in the beginning of exposure for slim slabs, as presented clearly in

Figure 8. Larger central opening sizes suffered more edge rotation, as a result of the lack of internal edge restraints. The 100 mm thick slabs behaved in a way resembling 50 mm, but by a smoother pattern, due to the lag in slab heating and the mild temperature distribution within the slab. Thicker slab behavior was much more different, where the 200 mm slab showed steady rotation value after 60 minutes, on the other hand increasing edge rotation for the case of 400 mm slab thickness. Edge rotation value kink appeared to delay in case of thicker slabs.

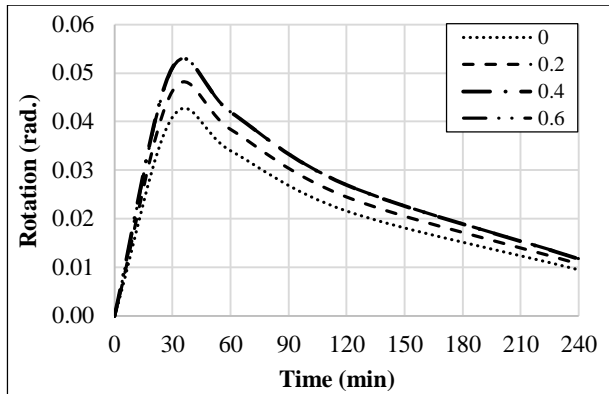


Figure 12. Edge rotation for 50mm slab, D/d=200

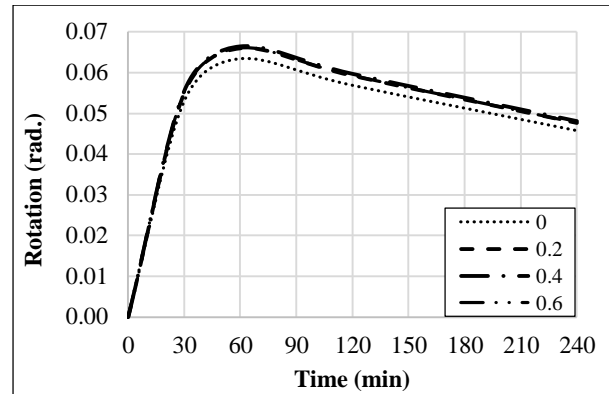


Figure 13. Edge rotation for 100mm slab, D/d=200

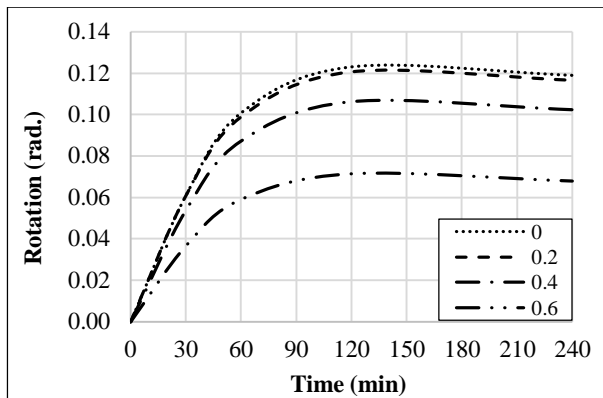


Figure 14. Edge rotation for 200mm slab, D/d=200

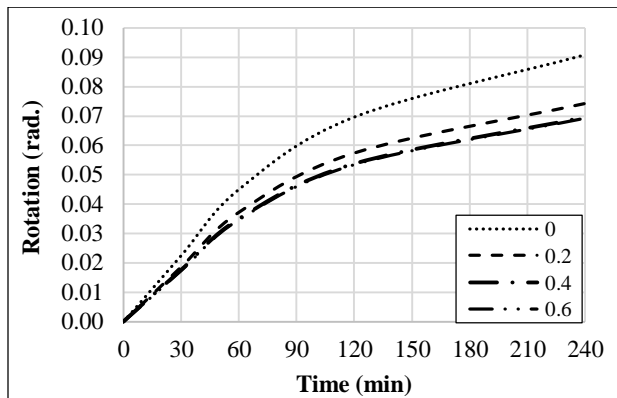


Figure 15. Edge rotation for 400mm slab, D/d=200

4.2. Thermal Induced Deflection Profile

Deflection profile has been extracted for solid slabs only. Wide slenderness spectrum ranging from $D/d = 25$ up to $D/d = 200$ has been investigated. Deflection profile has been expressed relative to slab diameter (Δ/D). It could be noticed that thermally induced deflection followed the same form as superimposed loads deflection. They are both non-linear and towards the gravity direction, since thermal load has been applied from slab soffit. It could be noticed the most influenced slabs regarding deflection are the intermediate slabs of depth in the order of 200 mm. Very deep slabs require a long exposure time till temperature increase reaches their upper side. That is why the 400 mm slab showed less deflection/ diameter ratio than 200 mm slab, for the 30 min exposure. On the other hand slim slabs temperature rises rapidly within the first 30 minutes, but with mild temperature variation through depth. Afterwards temperature becomes almost uniform within the slab depth. That is why thermally induced deflection decreases by increase in exposure time. Moreover thermally induced deflection behaves the same as structural induced, regarding effects of slenderness. The more the slenderness ration the more the more the deflection relative to diameter. It could also be noticed that the band width of thermally induced deflection with time increases for thicker slabs than thinner ones; which means that deflection is more vulnerable to variation in temperature across the cross section, than material deterioration, resulting from increase in mean temperature.

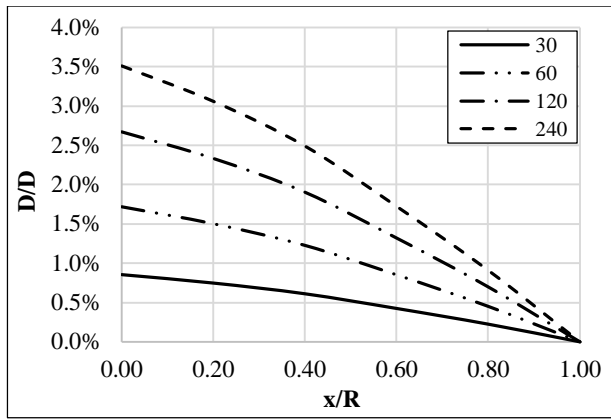


Figure 16. Deflection profile for 400 mm slab, $D/d=200$

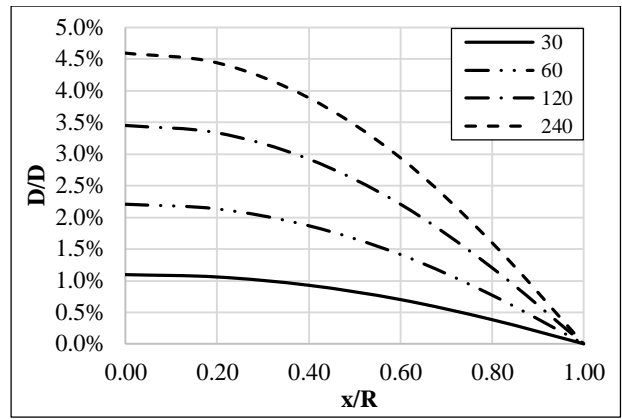


Figure 17. Deflection profile for 400 mm slab, $D/d=100$

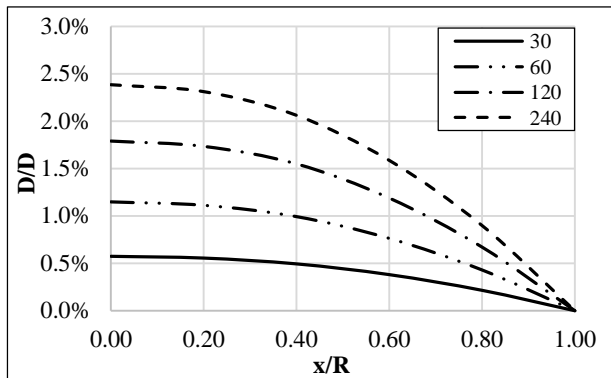


Figure 18. Deflection profile for 400mm slab, $D/d=50$

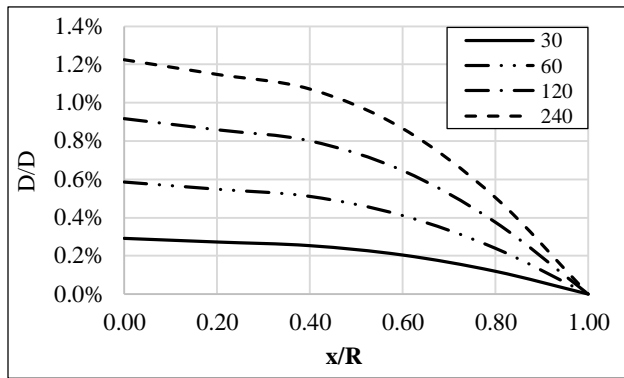


Figure 19. Deflection profile for 400mm slab, $D/d=25$

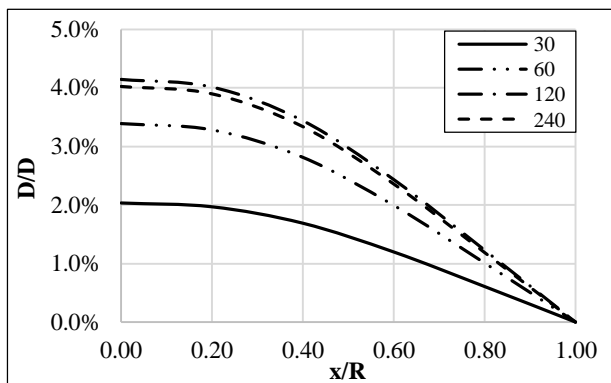


Figure 20. Deflection profile for 200mm slab, $D/d=200$

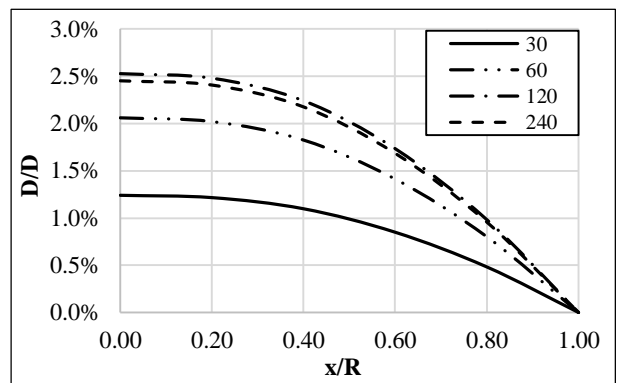


Figure 21. Deflection profile for 200mm slab, $D/d=100$

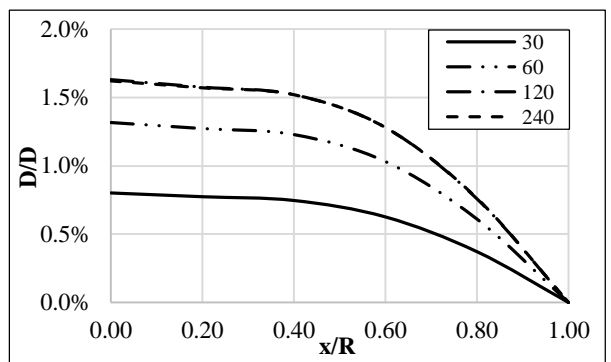


Figure 22. Deflection profile for 200mm slab, $D/d=50$

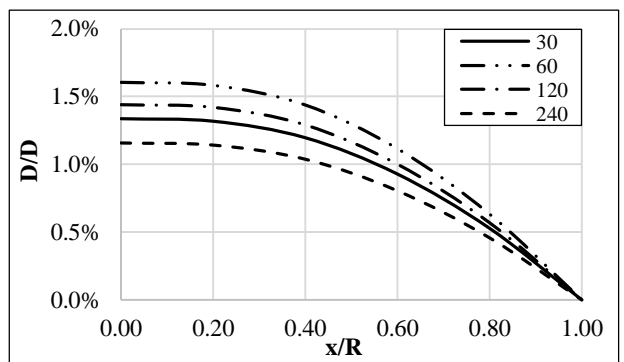


Figure 23. Deflection profile for 100mm slab, $D/d=200$

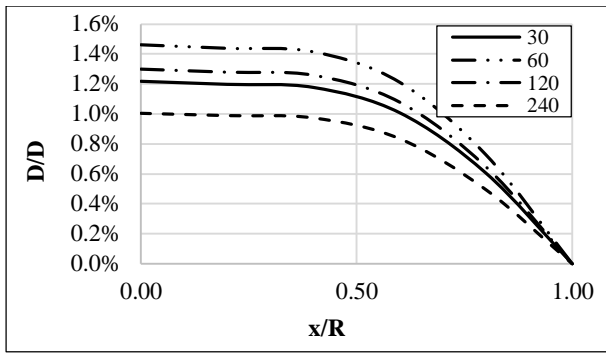


Figure 24. Deflection profile for 100mm slab, D/d=100

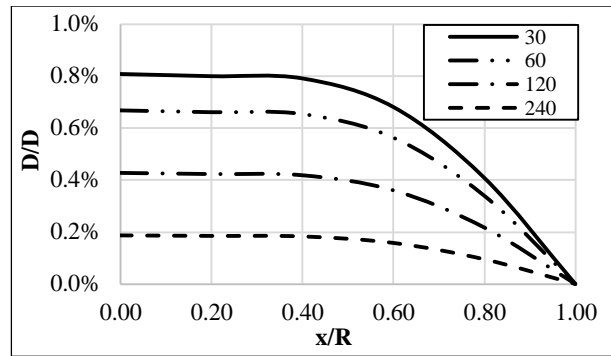


Figure 25. Deflection profile for 50mm slab, D/d=200

4.3. Thermal-Structural Relative Edge Rotation

The interaction between thermal and structural loading patterns is the most significant case to be studied, because it is the actual case that takes place in reality. Thermal-structural interaction has been studied through applying the loading curve stated before in Figure 3. Different practical structural load ratios have been considered beginning by 10%, passing by 30% and reaching 50%.

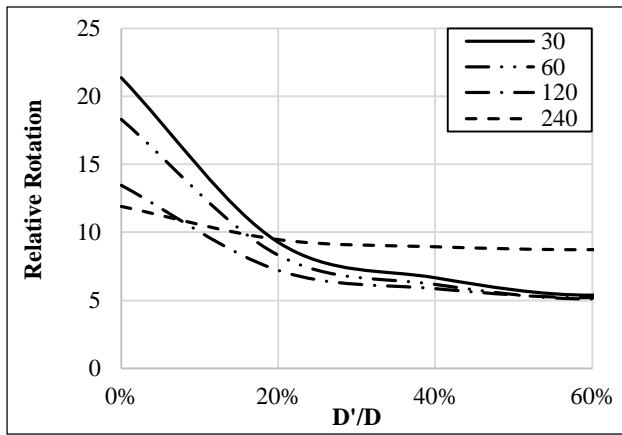


Figure 26. Relative edge rotation [d. 50mm, D/d. 200, L.R. 10%]

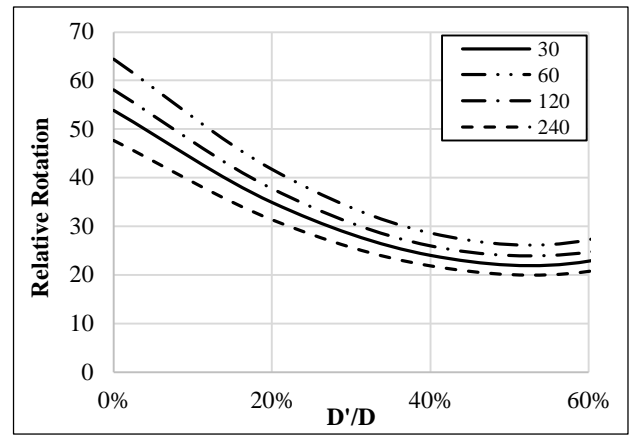


Figure 27. Relative edge rotation [d. 100mm, D/d. 200, L.R. 10%]

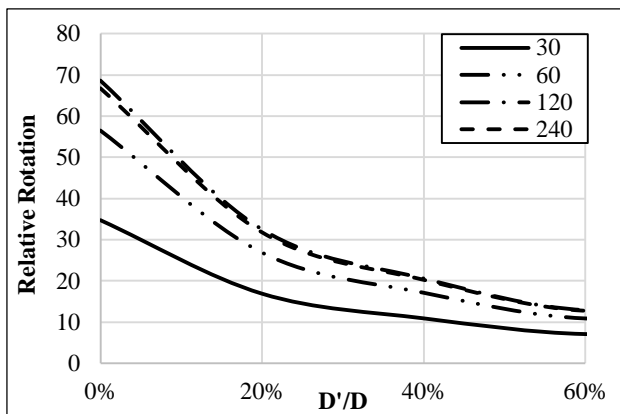


Figure 28. Relative edge rotation [d. 200mm, D/d. 200, L.R. 10%]

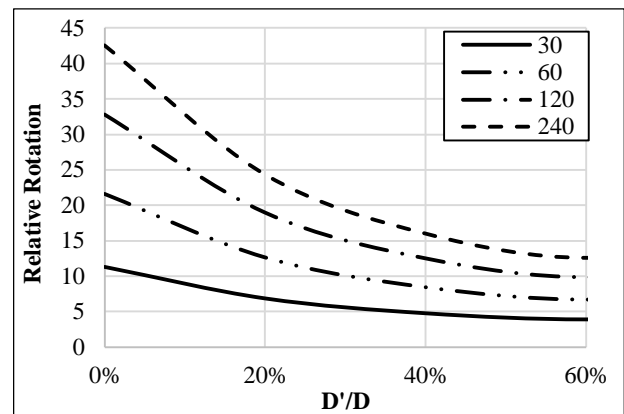


Figure 29. Relative edge rotation [d. 400mm, D/d. 200, L.R. 10%]

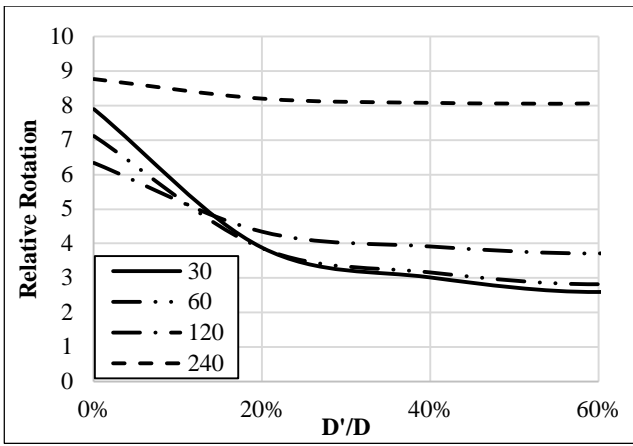


Figure 30. Relative edge rotation [d. 50mm, D/d. 200, L.R. 30%]

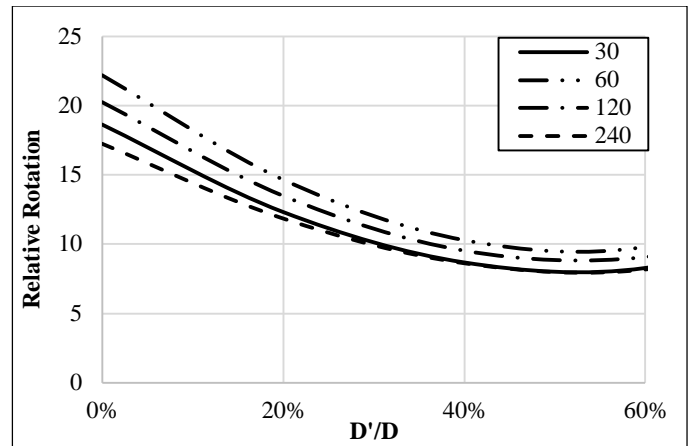


Figure 31. Relative edge rotation [d. 100mm, D/d. 200, L.R. 30%]

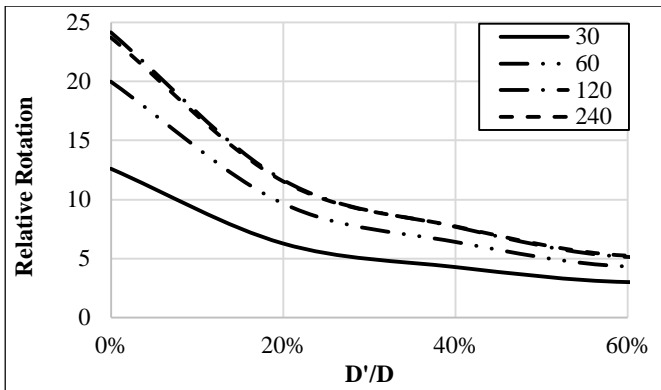


Figure 32. Relative edge rotation [d. 200mm, D/d. 200, L.R. 30%]

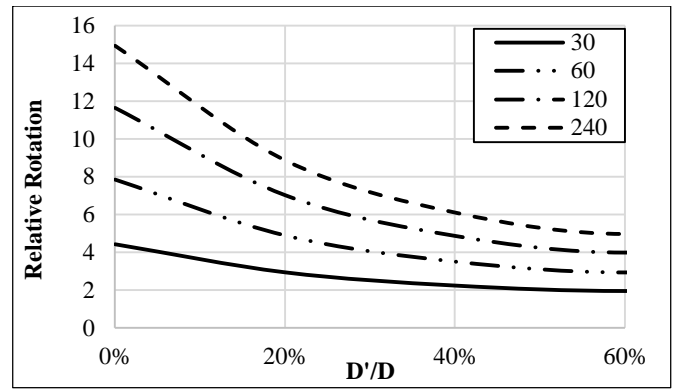


Figure 33. Relative edge rotation [d. 400mm, D/d. 200, L.R. 30%]

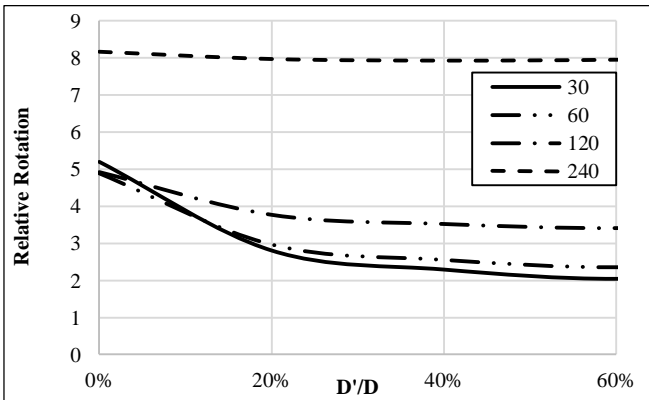


Figure 34. Relative edge rotation [d. 50mm, D/d. 200, L.R. 50%]

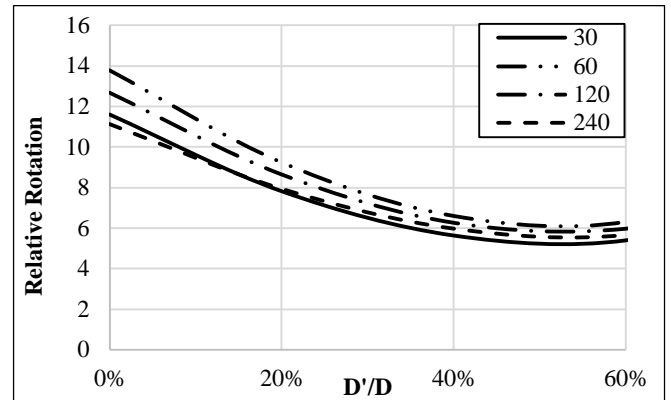


Figure 35. Relative edge rotation [d. 100mm, D/d. 200, L.R. 50%]

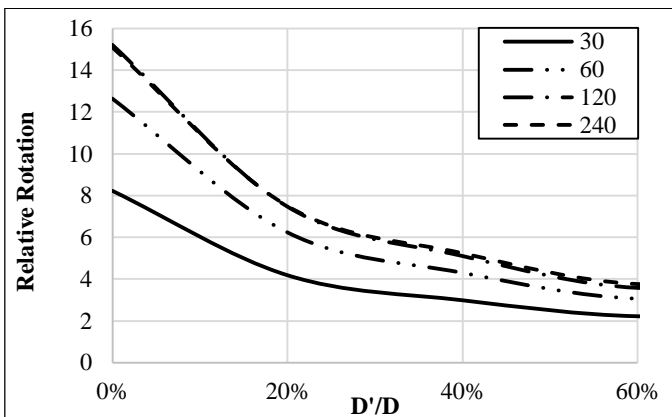


Figure 36. Relative edge rotation [d. 200mm, D/d. 200, L.R. 50%]

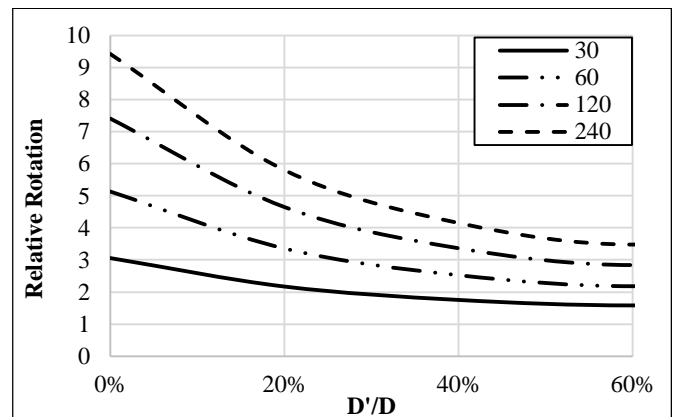


Figure 37. Relative edge rotation [d. 400mm, D/d. 200, L.R. 50%]

Exploring thermal-structural interaction has been performed through presenting combined edge rotation relative to structural edge rotation at the considered load ratio. It could be noticed that relative effect of thermal loading decreases by the increase in structural load ratio, in an approximately linear pattern. Moreover it could be noticed that relative edge rotation is about to be steady for the 50 mm deep slabs after a long period of fire exposure.

5. Conclusion

Outputs of the research could be divided to two categories. The first takes into account deformations, resulting from thermal load only; while the second considers thermal-structural interaction.

a) Thermal deformations

- 1) The more the span to depth ratio the more the mid-span deflection, resulting from thermal load only.
- 2) The more the span to depth ratio the more the difference in deflection to diameter ratio for different fire exposure time.
- 3) The ratio of deflection to diameter is forwardly proportional to time for deep slabs and inversely proportional for slim ones.
- 4) Deflection behaviour for slabs of thickness 10 mm or less differs significantly from that of slabs of thickness 200 mm or more.
- 5) Rate of increase in edge rotation is high in the first 30 minutes for 50 mm slabs, while in the first 60 minutes for thick slabs of fire exposure, as a result of retardation in thick slabs heating.
- 6) Slim slabs edge rotation drops after the first peak; while thick ones continue increasing, but with a lower rate.
- 7) The more the opening to diameter ratio the more the edge rotation for slim slabs and the less for thick slabs.

b) Thermal-structural interaction

- 1) The more the opening to diameter ratio the less the relative edge rotation (resulting from structural and thermal loads compared to that resulting from structural loads only).
- 2) The less the structural load ratio the wider the band width of relative edge rotation variation, as a function of exposure time.
- 3) Slab edge relative rotation is highly vulnerable to both sectional average and variation in temperature.

6. References

- [1] Alipour, M.M. 2016. "A Novel Economical Analytical Method For Bending And Stress Analysis Of Functionally Graded Sandwich Circular Plates With General Elastic Edge Conditions, Subjected To Various Loads". *Composites Part B: Engineering* 95: 48-63. doi:10.1016/j.compositesb.2016.03.090.
- [2] Reddy, Antonio Loya. 2016. "Nonlinear finite element analysis of functionally graded circular plates with modified couple stress theory". *European Journal of Mechanics - A/Solids* 56: 92-104. doi.org/10.1016/j.euromechsol.2015.11.001
- [3] Gaikwad, Kishor R. 2015. "Mathematical Modelling and Its Simulation of A Quasi-Static Thermoelastic Problem in A Semi-Infinite Hollow Circular Disk Due To Internal Heat Generation". *Journal of the Korea Society for Industrial and Applied Mathematics* 19 (1): 69-81. doi:10.12941/jksiam.2015.19.069.
- [4] Ghavami P. "Mechanics of Materials" (2015). Doi.org/ 10.1007/978-3-319-07572-3
- [5] Zi, Goangseup, Jihwan Kim, and Zdeněk P. Bažant. 2014. "Size Effect on Biaxial Flexural Strength of Concrete". *ACI Materials Journal* 111 (3). doi:10.14359/51686576.
- [6] Gaikwad, Kishor R. 2013. "Analysis of Thermoelastic Deformation of a Thin Hollow Circular Disk Due To Partially Distributed Heat Supply". *Journal of Thermal Stresses* 36 (3): 207-224. doi:10.1080/01495739.2013.765168.
- [7] FOSTER, S, I BURGESS, and R PLANK. 2005. "Investigation of Membrane Action in Model Scale Slabs Subject To High Temperatures". *Fourth International Conference on Advances in Steel Structures*, 933-940. doi:10.1016/b978-008044637-0/50138-4.
- [8] Elghazouli, A. Y., and B. A. Izzuddin. 2004. "Realistic Modeling Of Composite And Reinforced Concrete Floor Slabs Under Extreme Loading. II: Verification and Application". *Journal of Structural Engineering* 130 (12): 1985-1996. doi:10.1061/(asce)0733-9445(2004)130:12(1985).
- [9] Izzuddin, B. A., X. Y. Tao, and A. Y. Elghazouli. 2004. "Realistic Modeling Of Composite And Reinforced Concrete Floor Slabs Under Extreme Loading. I: Analytical Method". *Journal of Structural Engineering* 130 (12): 1972-1984. doi:10.1061/(asce)0733-9445(2004)130:12(1972).
- [10] Ma, L.S., and T.J. Wang. 2004. "Relationships Between Axisymmetric Bending And Buckling Solutions Of FGM Circular Plates

- Based On Third-Order Plate Theory And Classical Plate Theory". *International Journal of Solids and Structures* 41 (1): 85-101. doi:10.1016/j.ijsolstr.2003.09.008.
- [11] Huang, Zhaohui, Ian W. Burgess, and Roger J. Plank. 2003. "Modeling Membrane Action of Concrete Slabs in Composite Buildings in Fire. I: Theoretical Development". *Journal of Structural Engineering* 129 (8): 1093-1102. doi:10.1061/(asce)0733-9445(2003)129:8(1093).
- [12] Huang, Zhaohui, Ian W. Burgess, and Roger J. Plank. 2003. "Modeling Membrane Action of Concrete Slabs in Composite Buildings in Fire. II: Validations". *Journal of Structural Engineering* 129 (8): 1103-1112. doi:10.1061/(asce)0733-9445(2003)129:8(1103).
- [13] Huang, Zhaohui, Ian W. Burgess, and Roger J. Plank. 2001. "The Influence of Tensile Membrane Action in Concrete Slabs on the Behaviour of Composite Steel-Framed Buildings In Fire". *Structures* 2001. doi:10.1061/40558(2001)86.
- [14] Ma, Zhongcheng, and Pentti Mäkeläinen. 2000. "Behavior of Composite Slim Floor Structures in Fire". *Journal of Structural Engineering* 126 (7): 830-837. doi:10.1061/(asce)0733-9445(2000)126:7(830).
- [15] Dancygier, S. P. Shaw, and L. M. Keer. 1990. "Tests of Model Reinforced Concrete Circular Slabs". *ACI Structural Journal* 87 (6). doi:10.14359/2924.
- [16] Teng H. Hsu "Structural Engineering and Applied Mechanics", Vol. III, 3rd edition 1988. doi: 10.1115/1.3265659
- [17] Harmathy. T.Z. and Sultan. M.A. 1988. "Correlation between the severities of the ASTM E119 and ISO 834 fire exposures". *Fire Safety Journal* 13 (2): 163-168. doi. org/10.1016/0379-7112(88)90011-2
- [18] Judith J. Stalnaker and Ernest C. Harris. 1987. "Behavior of a Thick Circular Reinforced Concrete Slab under Two-Way Bending". *ACI Structural Journal* 84 (2). doi:10.14359/2795.
- [19] Lewis, G.K. 1968. "Shape Factors In Conduction Heat Flow For Circular Bars And Slabs With Various Internal Geometries". *International Journal of Heat and Mass Transfer* 11 (6): 985-992. doi:10.1016/0017-9310(68)90004-5.
- [20] Sawczuk, Antoni, and Lech Winnicki. 1965. "Plastic Behavior of Simply Supported Reinforced Concrete Plates at Moderately Large Deflections". *International Journal of Solids and Structures* 1 (1): 97-111. doi:10.1016/0020-7683(65)90019-3.
- [21] Hopkins, H.G., and W. Prager. 1953. "The Load Carrying Capacities of Circular Plates". *Journal of the Mechanics and Physics of Solids* 2 (1): 1-13. doi:10.1016/0022-5096(53)90022-2.